Electronic Supplemental Information

Biogenic nano-particulate iron-sulfide produced through sulfate and Fe(III)-(hydr)oxide reductions was enhanced by pyruvate as the electron donor

Chen Zhou[1]*, Zhuolin Liu[1], Pat Pataranutaporn[1], Raveender Vannela[1], Kim F. Hayes[2], and Bruce E. Rittmann[1]

[1] Swette Center for Environmental Biotechnology, Biodesign Institute, Arizona State University, USA

[2] Department of Civil and Environmental Engineering, University of Michigan, USA

*Corresponding author

Present address: Swette Center for Environmental Biotechnology, Biodesign Institute, Arizona State University, Tempe, AZ 85207-5701, USA

Tel: +01-480-634-3755

Email: zhou_SCEB@asu.edu

Procedure of mass-distribution calculations

To compute the distribution of Fe and S masses at the end of each experiment with solid-phase Fe, we developed a spreadsheet-based mass-balance and equilibrium model based on the approach of Tang, et al. [1].

The first principle of the model is mass balance for all components. The molar mass balances for all species of sulfur, carbonate, phosphate, citrate, and ammonia are in eqns. S1-S5, respectively:

$$C_{S^{2-},\,\text{free}}\left(V_g + V_l\right) = C_{H_2S_{(g)}} \cdot V_g + \left(\left[H_2S\right] + \left[HS^-\right] + \left[S^{2-}\right]\right) V_l \quad (S1)$$

$$C_{CO_2,\,\text{total}}\left(V_g + V_l\right) = C_{CO_{2(g)}} \cdot V_g + \left(\left[CO_2\right] + \left[HCO_3^-\right] + \left[CO_3^{2-}\right]\right) V_l \quad (S2)$$

$$C_{PO_4,\,\text{total}} = \left[H_3PO_4\right] + \left[H_2PO_4^-\right] + \left[HPO_4^{2-}\right] + \left[PO_4^{3-}\right] \quad (S3)$$

$$C_{\text{Cit, total}} = \left[H_3\text{Cit}\right] + \left[H_2\text{Cit}^-\right] + 2\left[H\text{Cit}^{2-}\right] + 3\left[\text{Cit}^{3-}\right] \quad (S4)$$

$$C_{NH_3,\,\text{total}}\left(V_g + V_l\right) = C_{NH_{3(g)}} \cdot V_g + \left(\left[NH_3\right] + \left[NH_4^+\right]\right) V_l \quad (S5)$$

where C_i is the total mole/L concentration of component i, [Xj] is the mole/L concentration of species j, V_g is the headspace volume, and V_l is the liquid volume. To take into account the gas-phase partitioning of CO_2, NH_3, and H_2S, we assumed equilibrium between their gas- and liquid-phase concentrations according to the "dimensionless" Henry's law constant (K_H) [2].

The second principle is that all of the acid/base reactions are at equilibrium, which is expressed quantitatively with mass-action equations and acidity constants (K_a). Eqns. S6 and S7 give an example of the mass-action equations for the NH_4^+/ NH_3 equilibrium of eqn. S5:

$$C_{NH_3\,(g)} = k_H\left(\left[NH_3\right] + \left[NH_4^+\right]\right) \quad (S6)$$

$$\left[NH_4^+\right] = k_a\left[NH_3\right] \quad (S7)$$

We did not make activity corrections, which means that we used mole/L concentration

in the mass-action equations.

The third principle of the model is that, at the end of the experiment (i.e., before we opened the bottles), the pH and alkalinity conform to the proton condition for all chemical species active in acid/base reactions:

$$\begin{aligned}\left[\mathrm{Alk}\right] &= \left[\mathrm{OH^-}\right] + \left[\mathrm{HS^-}\right] + 2\left[\mathrm{S^{2-}}\right] + \left[\mathrm{HCO_3^-}\right] + 2\left[\mathrm{CO_3^{2-}}\right] + \left[\mathrm{H_2PO_4^-}\right] + 2\left[\mathrm{HPO_4^{2-}}\right] \\ &\quad + 3\left[\mathrm{PO_4^{3-}}\right] + \left[\mathrm{H_2Cit^-}\right] + 2\left[\mathrm{HCit^{2-}}\right] + 3\left[\mathrm{Cit^{3-}}\right] - \left[\mathrm{H^+}\right] - \left[\mathrm{NH_4^+}\right] \\ &= \left[\mathrm{Na^+}\right] + \left[\mathrm{K^+}\right] + 2\left[\mathrm{Ca^{2+}}\right] + 2\left[\mathrm{Mg^{2+}}\right] + 2\left[\mathrm{Fe^{2+}}\right] - \left[\mathrm{Cl^-}\right] - 2\left[\mathrm{SO_4^{2-}}\right] \\ &\quad - \left[\mathrm{Lac^-}\right] - \left[\mathrm{Ac^-}\right] \end{aligned} \quad (S8)$$

where Alk stands for alkalinity, Cit stands for citrate, Lac stands for lactate, and Ac stands for acetate.

We made a few assumptions to simplify the model:

1. Total concentrations of non-transformed components in the original medium (citrate, calcium, magnesium, chloride, sodium, and potassium) were constant throughout the experiments.
2. The very small uptakes of ammonium and phosphate for bacterial synthesis [3] were neglected.
3. Lactate fermentation produced an equal concentration of total carbonate （i.e., $C_{CO2,\ total} = \Delta[\text{lactate}]$).

To solve the model, we applied the following input concentrations from our measurements:

- $[\text{sulfate}]_{final}$
- $[Fe^{2+}]_{final}$
- pH_{final}
- Organic compounds: $[Lac]_{final}$, $[Ac]_{final}$, and $[Cit]_{toal}$
- $C_{CO2,\ total}$
- Other inorganic ions: ($[Na^+]$, $[NH_4^+]$, $[Ca^{2+}]$, $[Mg^{2+}]$, and $[Cl^-]$).

To yield the output of $C_{s2-,\ free}$, we set up the *solver*, an add-in program in Excel, to iterate eqn. S8 for $C_{s2-,\ free}$ until the targeted pH equaled the measured pH on the

basis of eqns. S1 – S8. With pH and $C_{S2,\ free}$ known, we then calculated C_{s0}, C_{FeS}, and $C_{Fe(III)\ (hydr)xodes,\ remaining}$ according to eqns. 10 – 12.

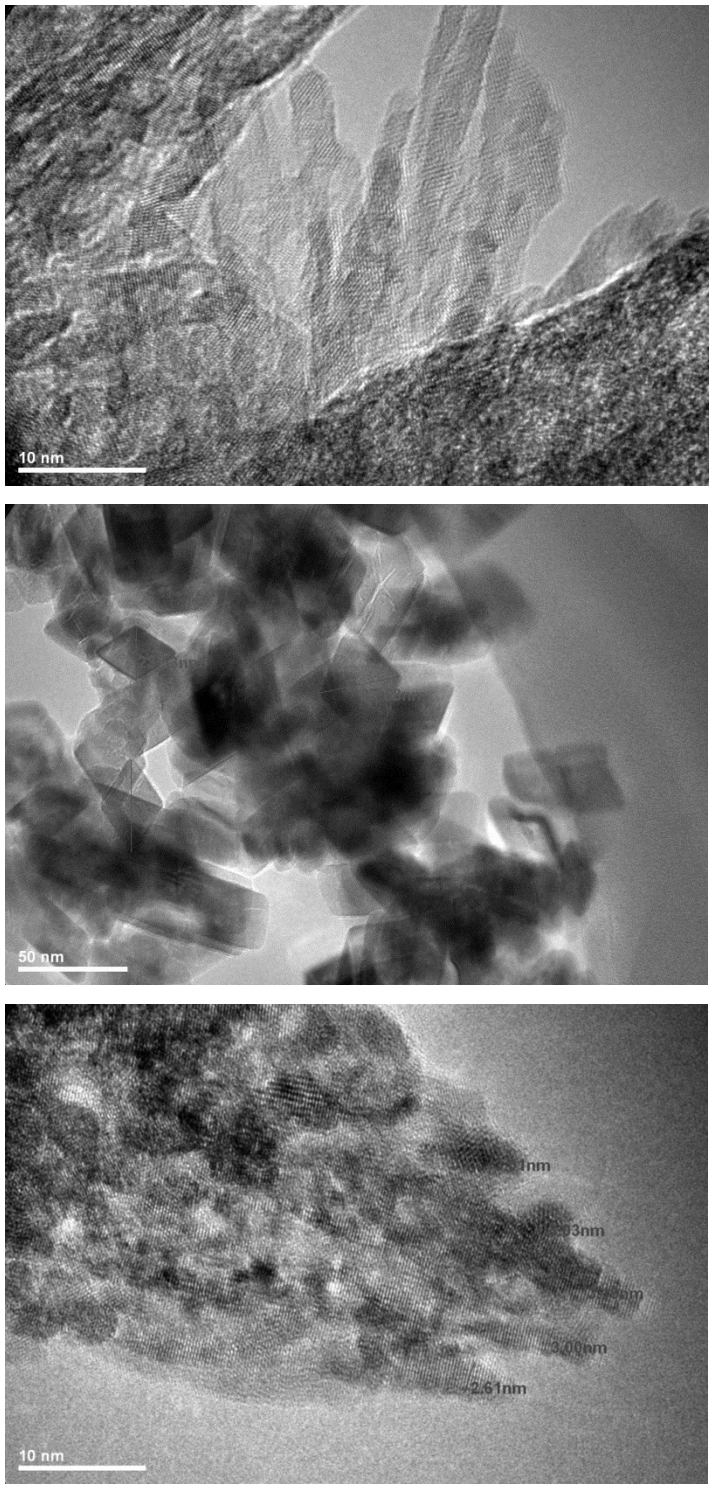

Figure S1. TEM images of synthetic nanoparticles of acicular-shaped goethite (top), diamond-shaped hematite (middle), and indistinctly edged 2-line ferrihydrite (bottom), with average sizes of (in nm) 6.6±1.4, 25.9±6.4, and3.5±1.5, respectively. These characteristics are similar to previous reports [4-8].

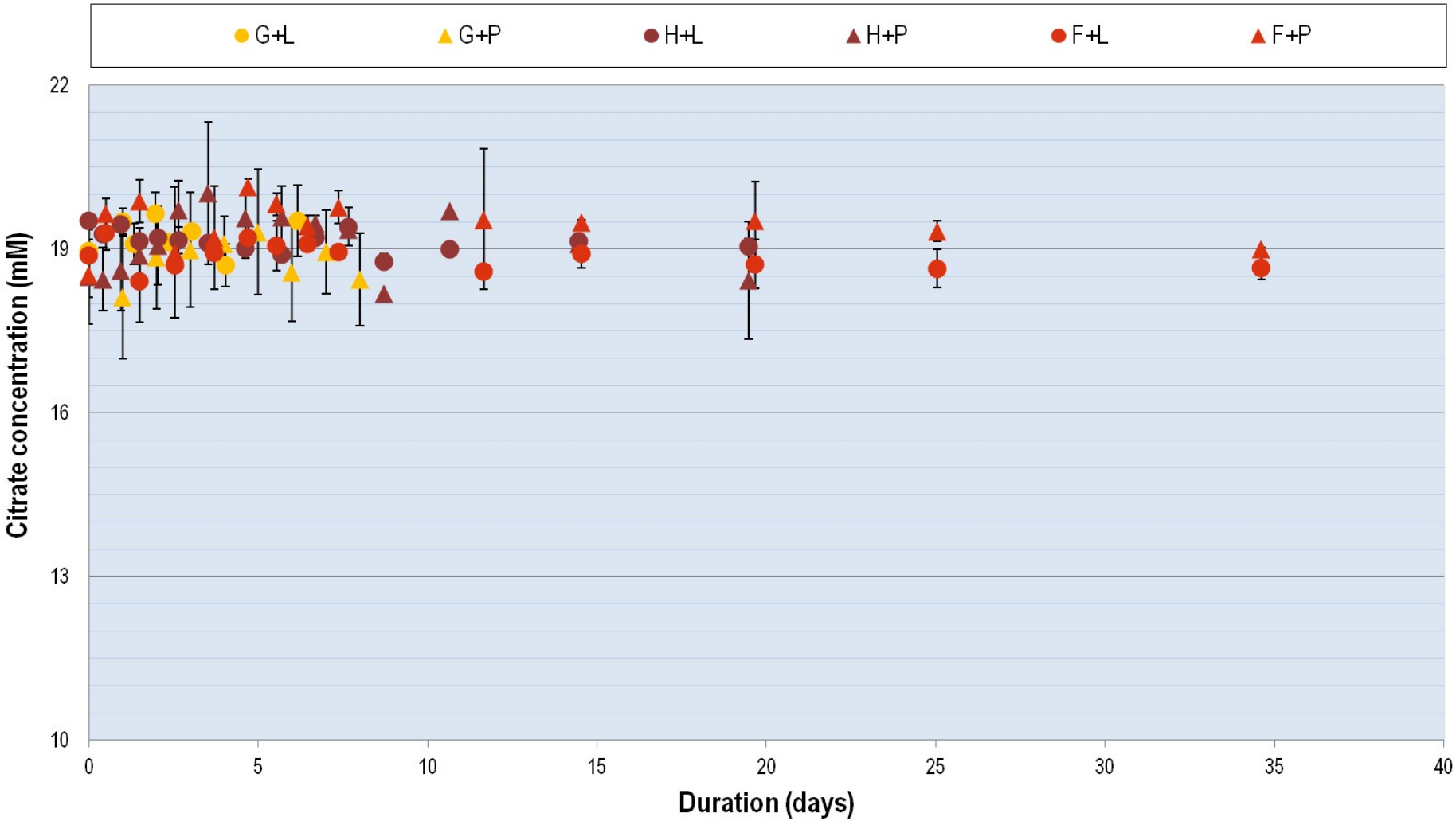

Figure S2. Citrate concentrations during incubation for all biotic conditions.

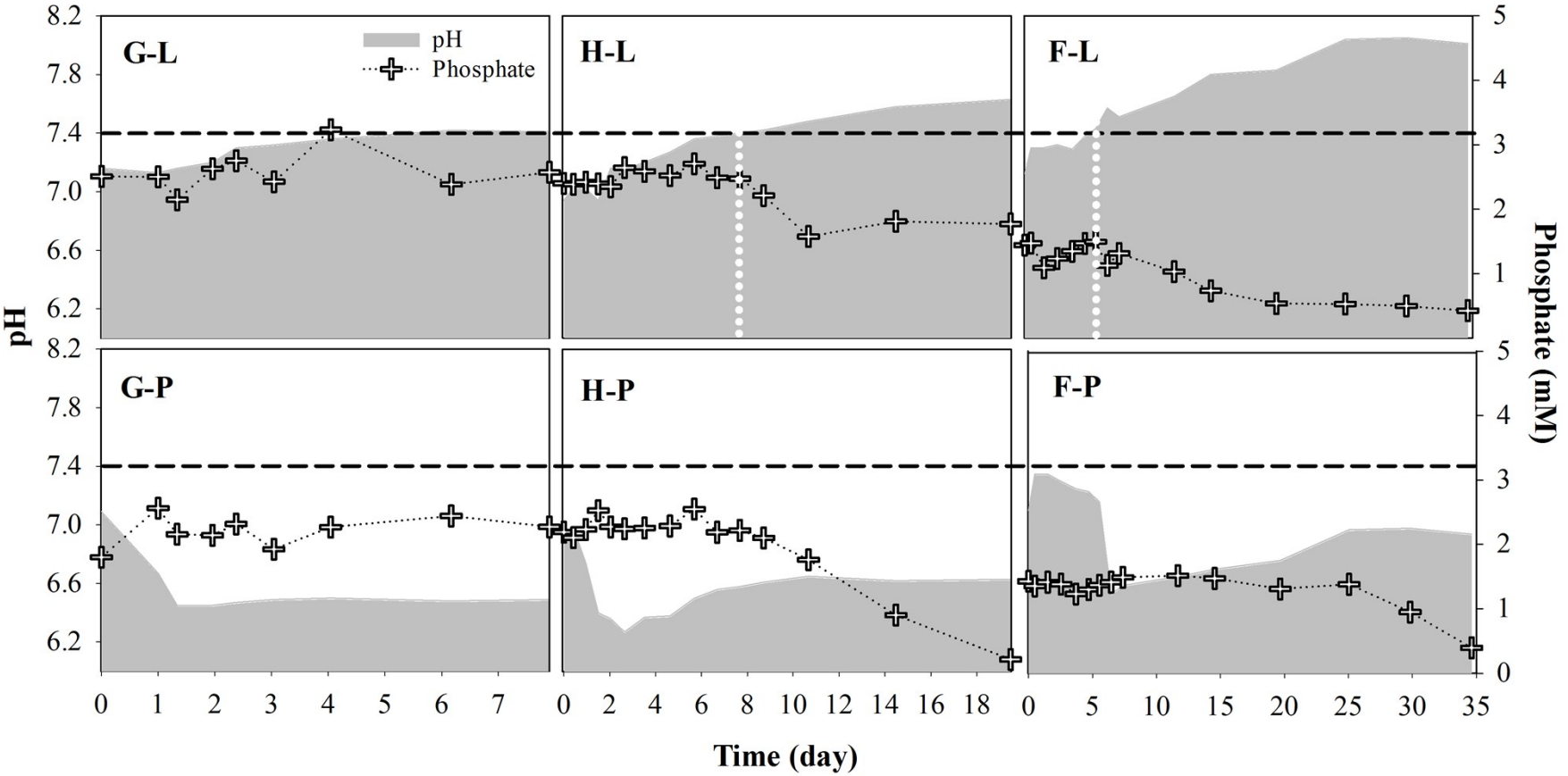

Figure S3. Phosphate concentrations and pH values during incubation in bottles containing goethite plus lactate (G-L), hematite plus lactate (H-L), 2-line ferrihydrite plus lactate (F-L), goethite plus pyruvate (G-P), hematite plus pyruvate (H-P), and 2-line ferrihydrite plus pyruvate (F-P). The horizontal black dash lines refer to the threshold value of pH (7.5) to allow Ca-PO_4 precipitation, as proposed by previous research[9, 10]. The vertical white dotted lines indicates the time when phosphate concentrations began to drop in the H-L and F-L bottles. These indicate a strong and precise correlation between pH and phosphate precipitation.

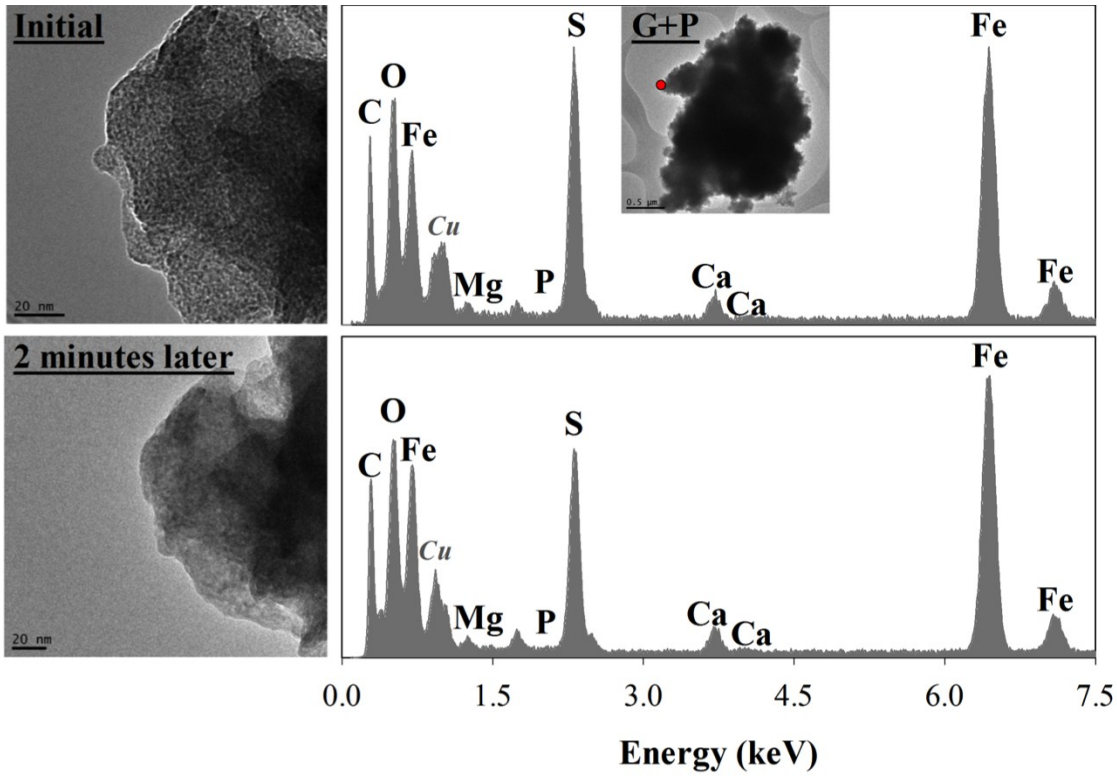

Figure S4. TEM images and EDX spectra of a single spot in the solids produced from the bottle with goethite plus pyruvate (G-P), taken at a magnification of 140,000× immediately and after 2 minutes. The shrinking area and the lowered S:Fe peak ratio indicates the loss of sulfur by the electron beams.

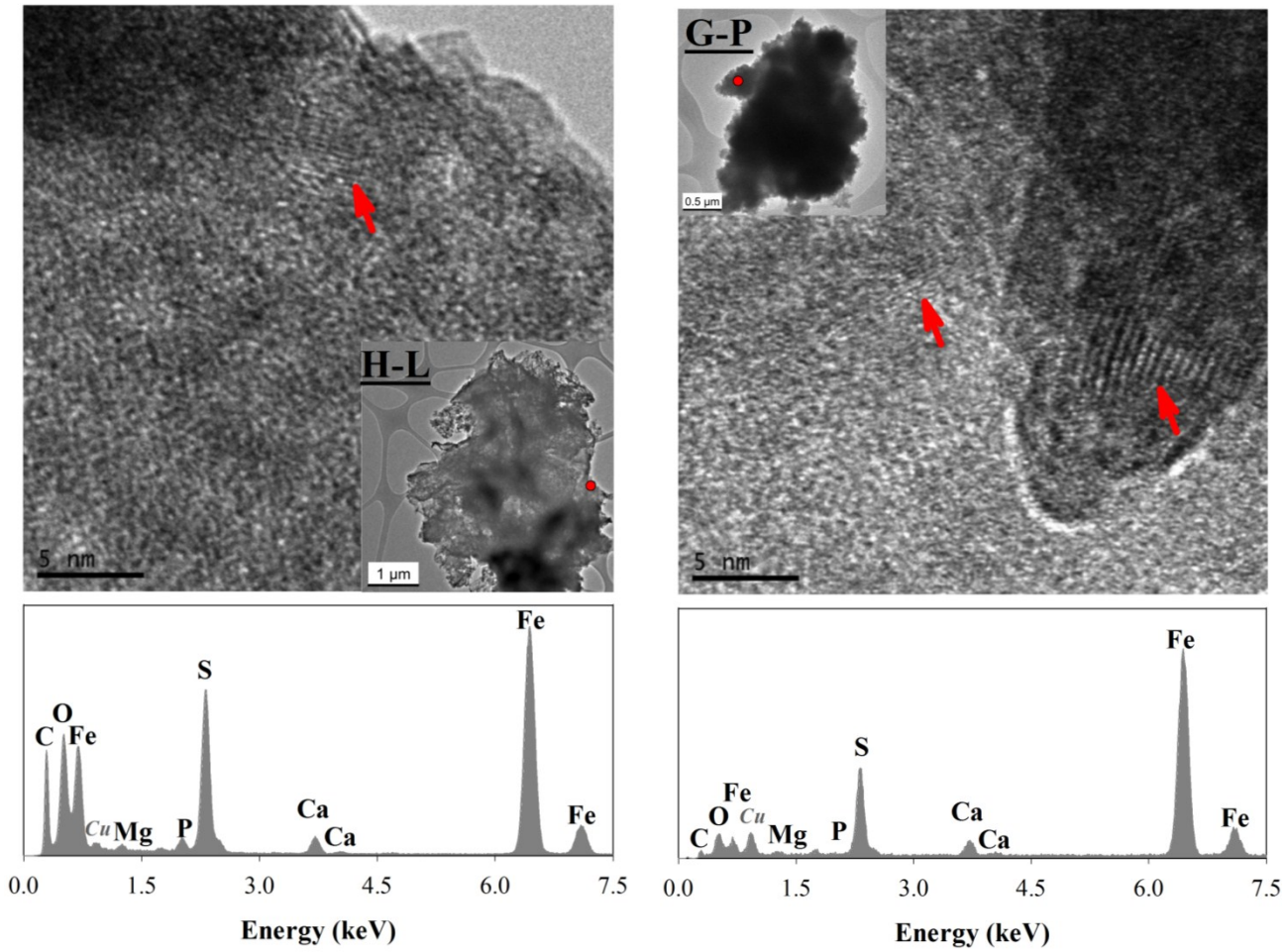

Figure S5. The TEM images and the EDX results of a nm-level spot showing crystal lattices in the solids from bottles with hematite plus lactate (H-L; left) and geothite plus pyruvate (G-P; right). Red dots indicate the selected areas, and red arrows indicate the lattice fringes.

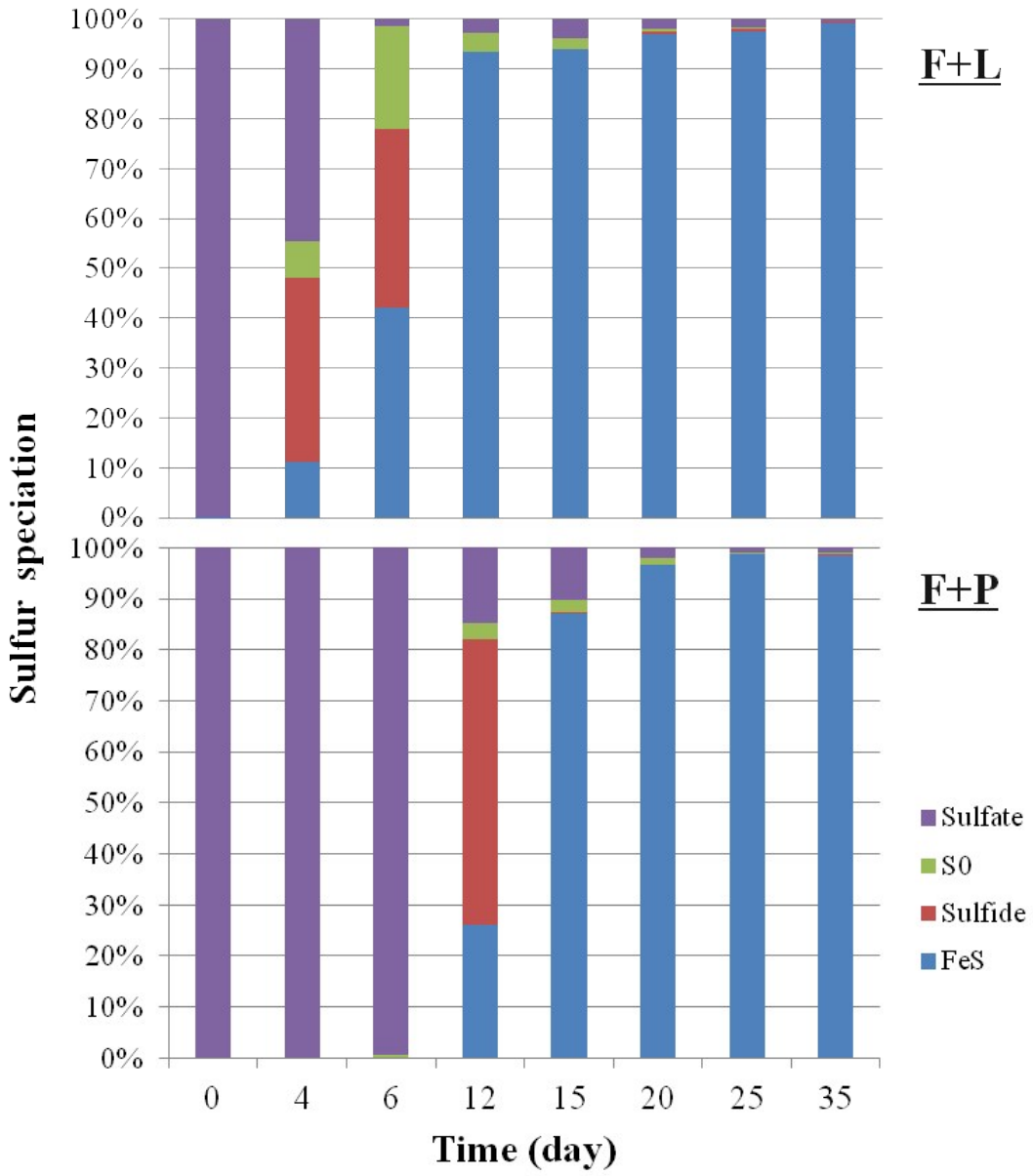

Figure S6. The sulfur speciation during the incubation period in the ferrihydrite bottles.

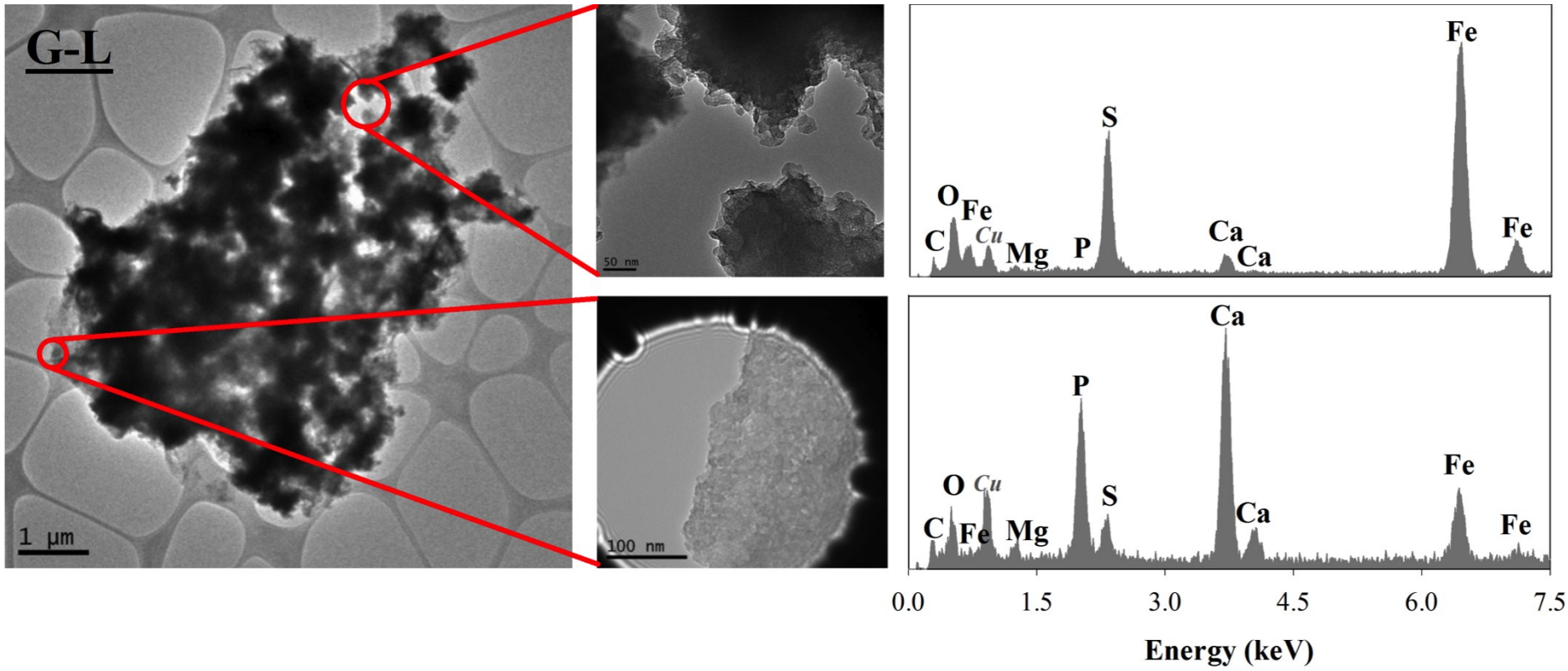

Figure S7. TEM images and the comprehensive EDX results of two spots in the solids produced from the bottle with goethite plus lactate (G-L). Ca and P have much higher intensities at the edge of the aggregate than inside the aggregate.

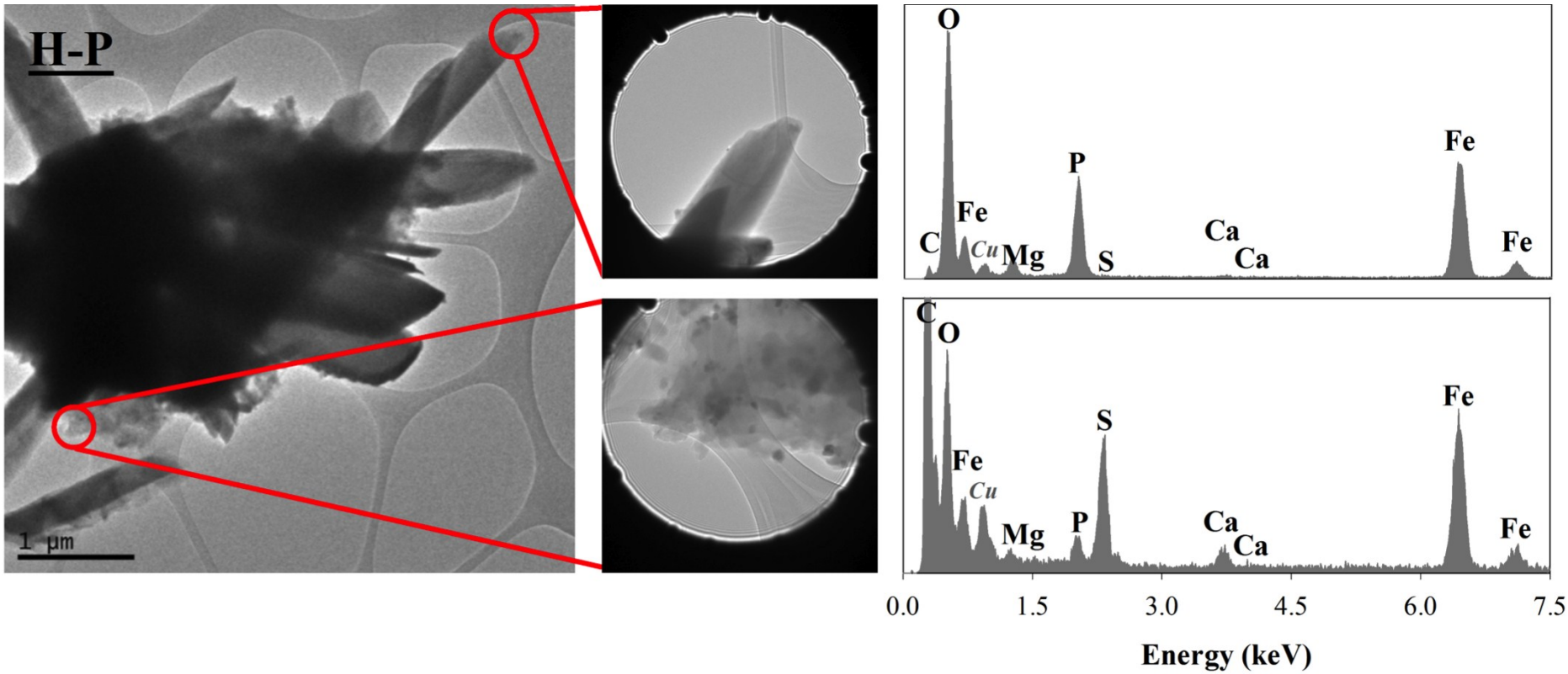

Figure S8. The TEM images and the comprehensive EDX results of two spots in the solids produced from the bottle with hematite plus pyruvate. The strong Fe and P signals but invisible S signal in the upper area indicates that the large slab-shpaed crstyals in μm level was vivianite, while the strong Fe and S signals in the lower area indicates that FeS solids mainly accumulated at the edge of vivianite clumps.

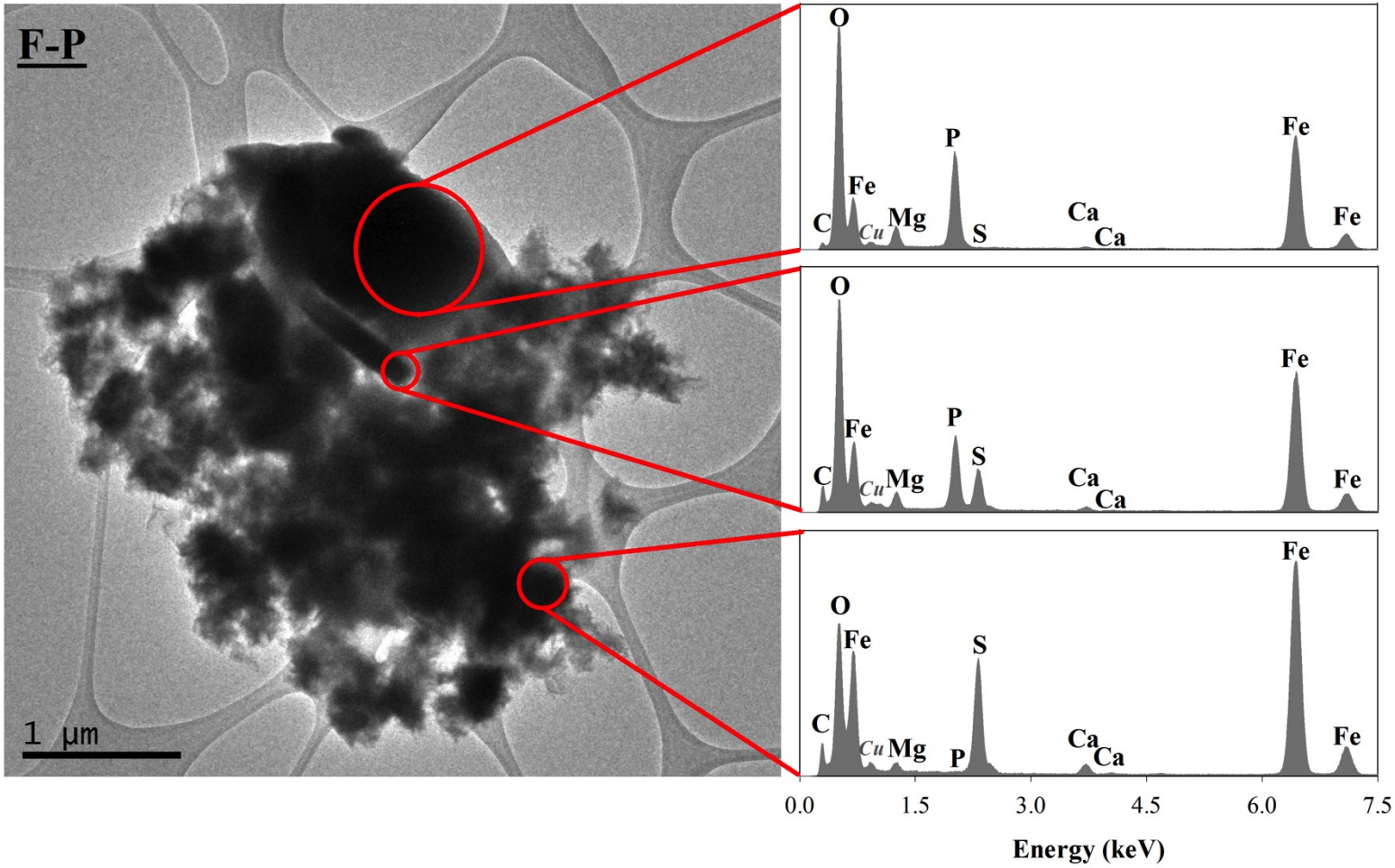

Figure S9. The TEM images and comprehensive EDX results for two spots in the solids produced from the bottle with hematite plus pyruvate. The bullet-shaped large crystals are proved to be vivianite, and the floc-like solids are mainly FeS.

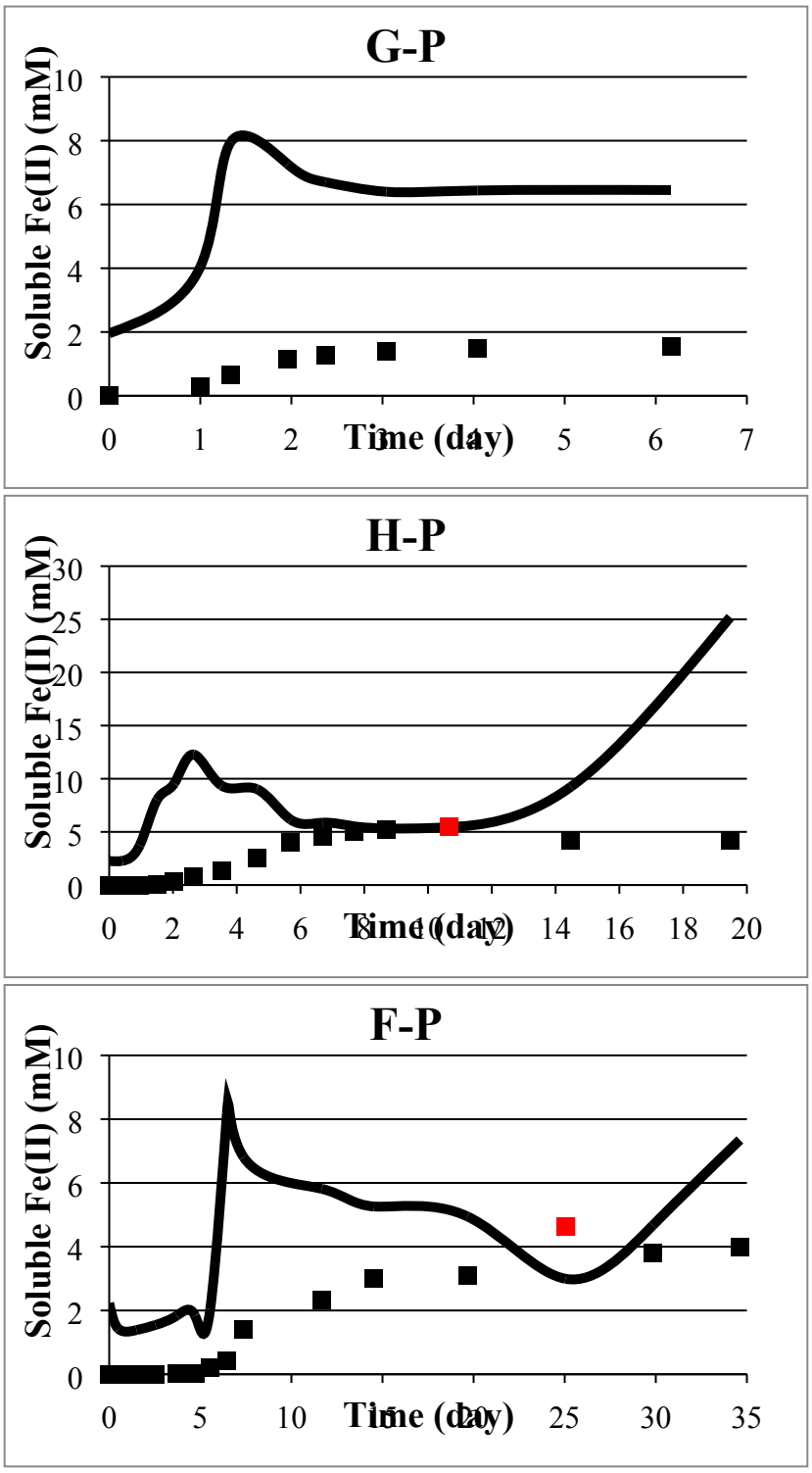

Figure S10. Solid lines: the simulated minimum soluble Fe(II) concentration allowing vivianite precipitation given the actual phosphate concentration and pH value in the G-P, H-P, and F-P bottles featuring 0.3 M inonic strength; Square dots: the actual soluble Fe(II) concentration in the G-P, H-P, and F-P bottles. The red dots represent the actual soluble Fe(II) concentrations above the simulated thresholds and thus causing vivianite formation.

References

1. Tang, Y.; Zhou, C.; Ziv-El, M.; Rittmann, B. E., A pH-control model for heterotrophic and hydrogen-based autotrophic denitrification. *Water Res* **2011,** *45*, (1), 232-240.
2. Snoeyink, V. L.; Jenkins, D., *Water chemistry*. Wiley: New York, 1980; p xiii, 463 p.
3. Noguera, D. R.; Brusseau, G. A.; Rittmann, B. E.; Stahl, D. A., A Unified Model Describing the Role of Hydrogen in the Growth of Desulfovibrio vulgaris under Different Environmental Conditions. *Biotechnol Bioeng* **1998,** *59*, (6), 732-746.
4. Dong, H. L.; Kukkadapu, R. K.; Fredrickson, J. K.; Zachara, J. M.; Kennedy, D. W.; Kostandarithes, H. M., Microbial reduction of structural Fe(III) in illite and goethite. *Environ Sci Technol* **2003,** *37*, (7), 1268-1276.
5. Kosmulski, M.; Durand-Vidal, S.; Maczka, E.; Rosenholm, J. B., Morphology of synthetic goethite particles. *J Colloid Interf Sci* **2004,** *271*, (2), 261-269.
6. Michel, F. M.; Ehm, L.; Antao, S. M.; Lee, P. L.; Chupas, P. J.; Liu, G.; Strongin, D. R.; Schoonen, M. A. A.; Phillips, B. L.; Parise, J. B., The structure of ferrihydrite, a nanocrystalline material. *Science* **2007,** *316*, (5832), 1726-1729.
7. Mohapatra, M.; Gupta, S.; Satpati, B.; Anand, S.; Mishra, B. K., pH and temperature dependent facile precipitation of nano-goethite particles in $Fe(NO_3)_3$-NaOH-$NH_3NH_2HSO_4$ · H_2O medium. *Colloid Surface A* **2010,** *355*, (1-3), 53-60.
8. Prelot, B.; Villieras, F.; Pelletier, M.; Gerard, G.; Gaboriaud, F.; Ehrhardt, J. J.; Perrone, J.; Fedoroff, M.; Jeanjean, J.; Lefevre, G.; Mazerolles, L.; Pastol, J. L.; Rouchaud, J. C.; Lindecker, C., Morphology and surface heterogeneities in synthetic goethites. *J Colloid Interf Sci* **2003,** *261*, (2), 244-254.
9. Ferguson, J. F.; Jenkins, D.; Eastman, J., Calcium Phosphate Precipitation at Slightly Alkaline pH Values. *J Water Pollut Con F* **1973,** *45*, (4), 620-631.
10. Ferguson, J. F.; Mccarty, P. L., Effects of Carbonate and Magnesium on Calcium Phosphate Precipitation. *Environ Sci Technol* **1971,** *5*, (6), 534-540.